

**Science**

 AAAS

**Iron Isotope Fractionation During Magmatic  
Differentiation in Kilauea Iki Lava Lake**

Fang-Zhen Teng, *et al.*  
*Science* **320**, 1620 (2008);  
DOI: 10.1126/science.1157166

***The following resources related to this article are available online at  
www.sciencemag.org (this information is current as of September 1, 2008 ):***

**Updated information and services**, including high-resolution figures, can be found in the online version of this article at:

<http://www.sciencemag.org/cgi/content/full/320/5883/1620>

**Supporting Online Material** can be found at:

<http://www.sciencemag.org/cgi/content/full/320/5883/1620/DC1>

A list of selected additional articles on the Science Web sites **related to this article** can be found at:

<http://www.sciencemag.org/cgi/content/full/320/5883/1620#related-content>

This article **cites 26 articles**, 3 of which can be accessed for free:

<http://www.sciencemag.org/cgi/content/full/320/5883/1620#otherarticles>

This article appears in the following **subject collections**:

Geochemistry, Geophysics

[http://www.sciencemag.org/cgi/collection/geochem\\_phys](http://www.sciencemag.org/cgi/collection/geochem_phys)

Information about obtaining **reprints** of this article or about obtaining **permission to reproduce this article** in whole or in part can be found at:

<http://www.sciencemag.org/about/permissions.dtl>

# Iron Isotope Fractionation During Magmatic Differentiation in Kilauea Iki Lava Lake

Fang-Zhen Teng,<sup>1\*</sup> Nicolas Dauphas,<sup>1</sup> Rosalind T. Helz<sup>2</sup>

Magmatic differentiation helps produce the chemical and petrographic diversity of terrestrial rocks. The extent to which magmatic differentiation fractionates nonradiogenic isotopes is uncertain for some elements. We report analyses of iron isotopes in basalts from Kilauea Iki lava lake, Hawaii. The iron isotopic compositions (<sup>56</sup>Fe/<sup>54</sup>Fe) of late-stage melt veins are 0.2 per mil (‰) greater than values for olivine cumulates. Olivine phenocrysts are up to 1.2‰ lighter than those of whole rocks. These results demonstrate that iron isotopes fractionate during magmatic differentiation at both whole-rock and crystal scales. This characteristic of iron relative to the characteristics of magnesium and lithium, for which no fractionation has been found, may be related to its complex redox chemistry in magmatic systems and makes iron a potential tool for studying planetary differentiation.

Studies of isotopic variations in terrestrial and extraterrestrial rocks can be used to identify the processes that govern planetary differentiation. For example, Fe isotopic compositions of lunar and terrestrial basalts are slightly heavier than those of chondrites, Mars, and Vesta; this has been ascribed to evaporation-induced kinetic fractionation of Fe isotopes during the giant impact that formed the Moon (1). This interpretation assumes that the Fe isotopic composition of basalts is representative of the source composition (i.e., mantle), which is supported by isotopic studies of other elements like Li and Mg (2, 3). Although studies of mantle peridotites have shown measurable Fe isotope fractionation during mantle melting (4, 5), the effect of fractional crystallization on Fe isotopes remains uncertain (6–10). Many processes—such as partial melting, magma mixing, assimilation of country rocks, fractional crystallization, and late-stage fluid exsolution—can affect Fe isotope systematics of the magma before it reaches the surface. Isotopic variations may result from different processes, and it is difficult to identify the contributions of specific processes to the observed isotopic signatures.

To isolate and evaluate the influence of fractional crystallization, we worked on a set of well-characterized samples from Kilauea Iki lava lake, Hawaii. Kilauea Iki lava lake formed during the 1959 summit eruption of Kilauea volcano by filling a previously existing crater (Fig. 1). After the formation of a stable crust at the end of the eruption, the lava lake cooled and crystallized as a small, self-roofed, closed magma chamber surrounded on all sides by partially molten regions and extending outward to fully solidified rocks

(11, 12). It was drilled repeatedly from 1960 to 1988, resulting in almost 1200 m of drill cores. We analyzed two 1959 eruption samples (IKI-22 and IKI-58) and a variety of drill core samples, ranging from olivine-rich cumulates to andesitic segregation veins, to cover the whole spectrum of chemical compositions, mineralogies, and crystallization temperatures (12).

The  $\delta^{56}\text{Fe}$  values  $\{\delta^{56}\text{Fe} = [(\frac{^{56}\text{Fe}}{^{54}\text{Fe}})_{\text{sample}} / (\frac{^{56}\text{Fe}}{^{54}\text{Fe}})_{\text{IRMM-014}} - 1] \times 1000\}$  of all the whole-

rock samples vary inversely with MgO and total FeO contents ( $\text{Fe}_2\text{O}_3$  and FeO calculated as  $\text{FeO}_{\text{total}}$ ) and directly with  $\text{Fe}^{3+}/\Sigma\text{Fe}$  ratios ( $\Sigma\text{Fe} = \text{Fe}^{3+} + \text{Fe}^{2+}$ ) (Fig. 2). Olivine cumulates have high MgO contents [up to 26.87 weight percent (wt %)] and low  $\delta^{56}\text{Fe}$  values (down to  $-0.03\%$ ), whereas late-stage veins have low MgO contents (down to 2.37 wt %) and high  $\delta^{56}\text{Fe}$  values (up to  $+0.22\%$ ) (table S1). The Fe isotopic compositions of 42 olivine grains, separated from two drill core samples, display a larger Fe isotopic variation, ranging from  $-1.10$  to  $+0.09\%$  (Fig. 3). The variations are irrespective of the olivine crystal weight (table S2). The average  $\delta^{56}\text{Fe}$  of these olivine grains is  $-0.22 \pm 0.08\%$  [95% confidence interval (CI)], which is significantly lower than that of the two whole rocks (i.e.,  $+0.11$  and  $+0.12\%$ ).

The large chemical variations in Kilauea Iki lavas mainly resulted from post-eruptive redistribution of olivine phenocrysts, followed by crystallization of pyroxene, plagioclase, and Fe-Ti oxide phases as the lava lake cooled (11). Both equilibrium (7, 8, 13, 14) and kinetic (15–17) Fe isotope fractionation between minerals and melts could happen during fractional crystallization and produce the observed Fe isotopic variations in the lava lake.

During the process of isotope fractionation, Fe isotopic variations in the samples with MgO < 11 wt %, which mainly result from fractional crystal-

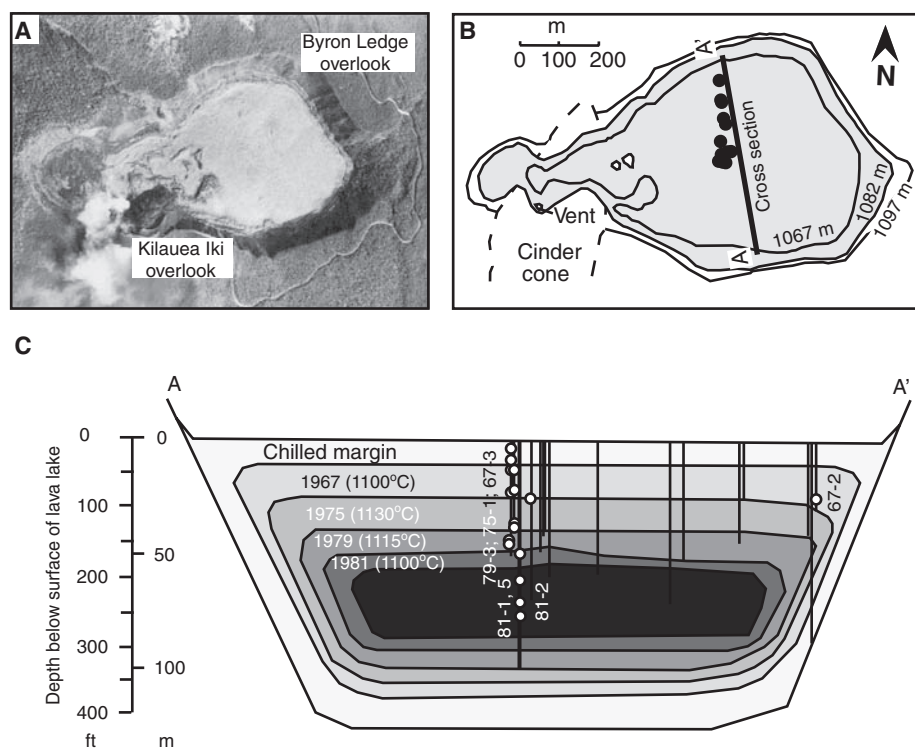


**Fig. 1.** (A) Aerial photograph (26) taken immediately after the 1959 eruption of Kilauea volcano, showing the surface of the newly formed Kilauea Iki lava lake. (B) Plan view of the post-eruptive surface of Kilauea Iki lava lake. The black circles indicate locations of holes drilled between 1967 and 1988. Numbers on contour lines are elevations above sea level. (C) Cross section of Kilauea Iki lava lake with a vertical exaggeration of 2:1. The vertical lines show locations of drill holes or closely spaced clusters of drill holes, projected onto this cross section. The concentric zones show the limit of drillable crust and temperatures at different years. Only the drill holes that are labeled indicate where samples (white circles) came from in this study.

<sup>1</sup>Origins Laboratory, Department of the Geophysical Sciences and Enrico Fermi Institute, University of Chicago, 5734 South Ellis Avenue, Chicago, IL 60637, USA. <sup>2</sup>United States Geological Survey, Reston, VA 20192, USA.

\*Present address: Isotope Laboratory, Department of Geosciences and Arkansas Center for Space and Planetary Sciences, University of Arkansas, 113 Ozark Hall, Fayetteville, AR 72701, USA.

†To whom correspondence should be addressed. E-mail: fteng@uark.edu

lization (11), can be modeled by Rayleigh fractionation with average crystal-melt fractionation factors ( $\Delta\delta^{56}\text{Fe}$ ) of  $\sim -0.1$  to  $-0.3\%$  (Fig. 4). For a

given  $\delta^{56}\text{Fe}$  of the original melt of  $\sim +0.1\%$ , the predicted  $\delta^{56}\text{Fe}$  of the minerals are  $\sim 0$  to  $-0.2\%$ . These values, in turn, are used to model the com-

positions of samples with  $\text{MgO} > 11$  wt %, which are composed of melt + olivine phenocrysts (11), by mixing the assumed composition of the most Mg-rich melt ( $\delta^{56}\text{Fe} = +0.11\%$ ) with that of the predicted olivine crystals ( $\delta^{56}\text{Fe} = 0$  to  $-0.2\%$ ) (Fig. 4) (12).

Although no experimentally calibrated equilibrium fractionation factor for olivine melt is currently available, the fractionation factors that fit the whole-rock data generally agree with theoretical calculations (13, 14), experimental studies on fractionation of pyrrhotite and silicate melt (7), and fractionation of olivine and magnetite (8). These results are also consistent with the range of Fe isotope fractionation during mantle melting (4, 5). However, olivine phenocrysts from the lava lake are highly varied and have  $\delta^{56}\text{Fe}$  values well beyond the range defined by the equilibrium isotope fractionation model (Fig. 4). Segregation veins and some diapirs are known to have formed as the lake crystallized (18). The diapirs transferred olivines from the cumulate zone into differentiated liquid (18). These processes affected the whole column of “mush” and could have magnified the equilibrium fractionation of Fe isotopes in the olivine in a way that is analogous to isotope fractionation during chromatography (19). Different olivine grains in the lake might have experienced these processes to different extents and hence display different degrees of isotope fractionation.

Alternatively, significant high-temperature kinetic fractionation of Mg and Fe isotopes has been documented during thermal diffusion in silicate melts (16, 17, 20) and chemical diffusion between molten basalt and rhyolite (16, 20). Substantial thermal gradients were observed in the lava lake throughout its crystallization history; the cumulate zone was hotter than the surrounding partially molten zone, and temperature gradients within the partially molten zone reached up to  $65^\circ\text{C}/\text{m}$  vertically (21). Because the hot end was always enriched with light isotopes during thermal diffusion experiments (16, 17, 20), these thermal gradients may have driven Fe diffusion and Fe isotope fractionation in both whole rocks and olivines, enriching the olivine cumulates in the light isotopes of Fe (and the light isotopes of Mg).

In addition to thermal diffusion, kinetic isotope fractionation can also happen by chemical diffusion. This could have happened during diffusion-limited crystal growth, where light isotopes can be supplied to the growing crystal at a faster rate than heavy isotopes resulting from differences in diffusivities (15, 22). Fractionation could also have taken place during chemical re-equilibration of olivines in the course of cooling and crystallization of the lava lake. The olivines from samples quenched at lower temperature are more Fe-rich and show more scatter in composition than those from samples quenched at higher temperature (fig. S1) (12), which reflects re-equilibration of the olivines with evolving residual melts (23). Diffusion of Fe from the melt into the interior of the olivine phenocrysts should be associated with kinetic isotope fractionation, thereby enriching the partially equilibrated

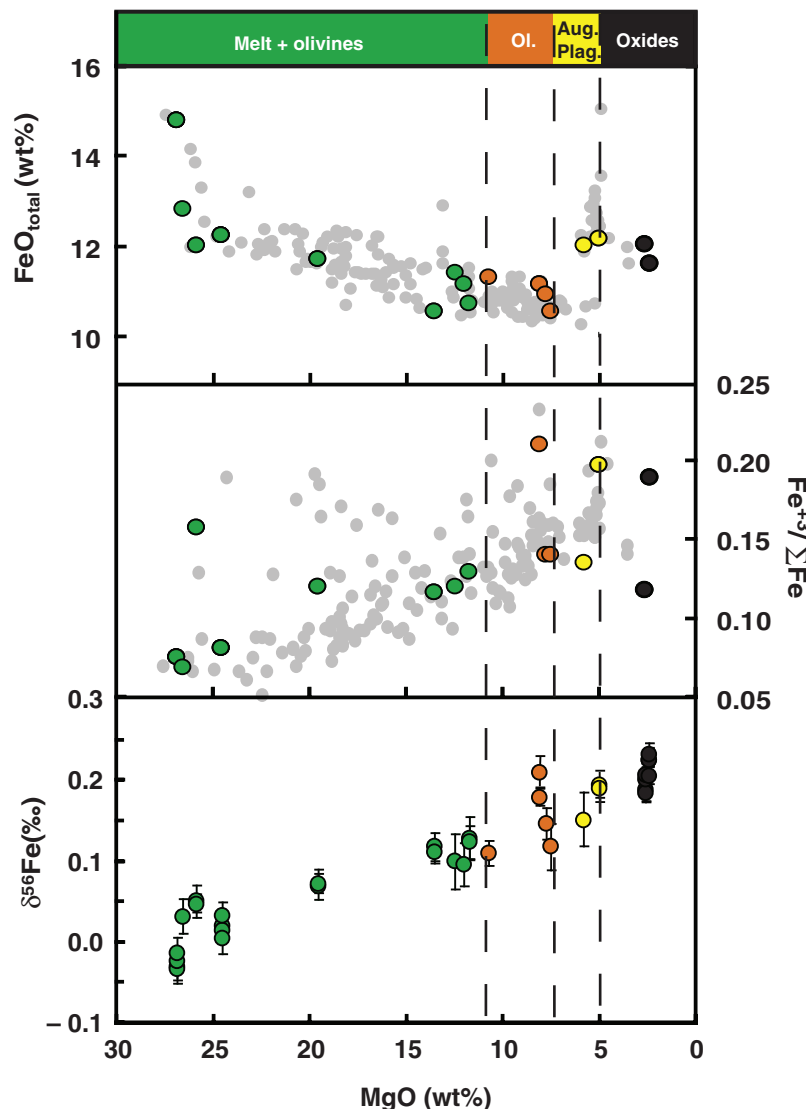


**Fig. 2.** Variations of  $\text{FeO}_{\text{total}}$ ,  $\text{Fe}^{3+}/\Sigma\text{Fe}$  ratios, and  $\delta^{56}\text{Fe}$  values as a function of MgO contents in whole-rock samples. Samples with  $\text{MgO} > 11$  wt % are melt + olivine phenocrysts, whereas those with  $\text{MgO} < 11$  wt % reflect fractional crystallization of olivine (Ol.), followed by augite (Aug.), plagioclase (Plag.), and Fe-Ti oxides (11). Gray circles represent all samples from Kilauea Iki lava lake (27). Error bars indicate 95% CI of the mean. Data from table S1.

**Fig. 3.** Iron isotopic compositions of olivine grains from Kilauea Iki lava lake. The curves are kernel density estimates with automatic bandwidth selection and have the same surface area. The dashed lines are the  $\delta^{56}\text{Fe}$  values ( $+0.11$  and  $+0.12\%$ ) of those two whole rocks. Error bars indicate 95% CI of the mean. Data from tables S1 and S2.

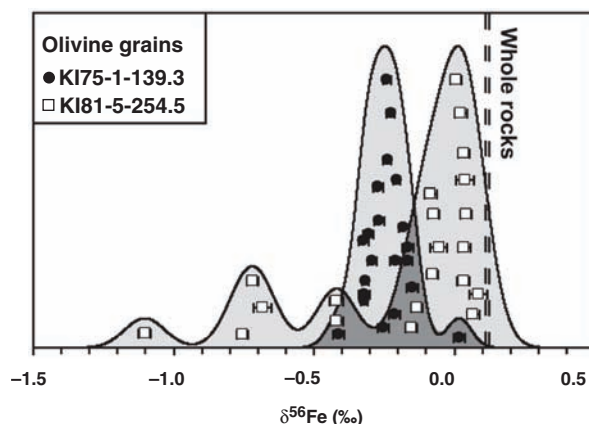
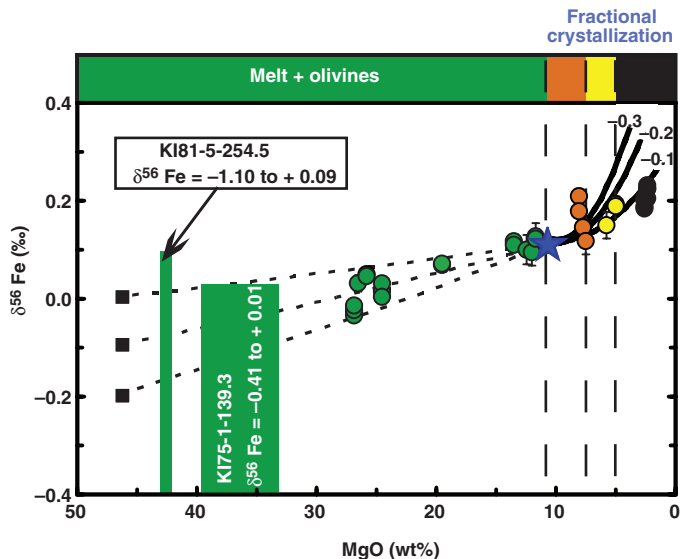


**Fig. 4.** Modeling of Fe isotopic variations during magmatic differentiation in Kilauea Iki lava lake (12). Solid lines represent calculated Fe isotopic compositions of residual melts during fractional crystallization by assuming a Rayleigh distillation process with average crystal-melt fractionation factors ( $\Delta\delta^{56}\text{Fe}_{\text{crystal-melt}} = \delta^{56}\text{Fe}_{\text{crystal}} - \delta^{56}\text{Fe}_{\text{melt}}$ ) of  $-0.1$ ,  $-0.2$ , and  $-0.3\text{‰}$ . Dashed horizontal lines represent calculated mixing lines between the most magnesian melt from the 1959 eruption (23) and the most magnesian olivines [(MgO =  $46.6 \pm 1$  wt % and  $\delta^{56}\text{Fe} = 0$ ,  $-0.1$ , and  $-0.2\text{‰}$ ) (black squares)]. The blue star represents the most magnesian melt (MgO = 10.7 wt %; assumed  $\delta^{56}\text{Fe} = 0.11\text{‰}$ ). The green bars represent the ranges of measured  $\delta^{56}\text{Fe}$  and estimated MgO in olivine grains from two drill core samples (MgO = 33.6 to 39.8 wt % and 41.9 to 42.7 wt %; table S3). Sample crystallization sequences are the same as those in Fig. 2. Error bars indicate 95% CI of the mean.



olivines in the light isotopes of Fe (and the heavy isotopes of Mg) (16, 20).

The extent of equilibrium isotope fractionation is mainly controlled by the relative mass difference between the isotopes, and more fractionation happens in isotopes with a larger relative mass difference (14, 24). If the Fe isotopic variation in the lava lake was produced by equilibrium isotope fractionation, Mg isotopes should show more significant fractionation than Fe isotopes because of their larger relative mass difference. Furthermore, kinetic isotope fractionation driven by thermal and chemical diffusion should also result in larger fractionation in Mg isotopes as compared with that in Fe isotopes (16, 17, 20). The absence of Mg isotope fractionation in Kilauea Iki lavas may result from the low-precision isotopic analysis of Mg relative to Fe (e.g., 0.1 versus 0.04), which prevents the detection of Mg isotopic variation. More likely, the presence of Fe isotope fractionation and the absence of Mg isotope fractionation may reflect the influence of Fe oxidation states on kinetic or equilibrium isotope fractionation (as compared with those of Mg, two oxidation states of Fe exist in terrestrial magmatic systems) (5, 25).

Our study suggests that, unlike Li and Mg isotopes (2, 3), Fe isotopes fractionate during basaltic differentiation at both whole-rock and crystal scales. Mineral compositions should therefore be used to help interpret whole-rock basalt Fe isotopic data. The elevated  $\delta^{56}\text{Fe}$  of crustal igneous rocks, which is more evolved than that in basalts, could be explained by fractional crystallization (10).

#### References and Notes

1. F. Poitrasson, A. N. Halliday, D. C. Lee, S. Levasseur, N. Teutsch, *Earth Planet. Sci. Lett.* **223**, 253 (2004).

2. F.-Z. Teng, M. Wadhwa, R. T. Helz, *Earth Planet. Sci. Lett.* **261**, 84 (2007).
3. P. B. Tomascak, F. Tera, R. T. Helz, R. J. Walker, *Geochim. Cosmochim. Acta* **63**, 907 (1999).
4. S. Weyer, D. A. Ionov, *Earth Planet. Sci. Lett.* **259**, 119 (2007).
5. H. M. Williams *et al.*, *Earth Planet. Sci. Lett.* **235**, 435 (2005).
6. B. L. Beard *et al.*, *Chem. Geol.* **195**, 87 (2003).
7. J. A. Schuessler, R. Schoenberg, H. Behrens, F. von Blanckenburg, *Geochim. Cosmochim. Acta* **71**, 417 (2007).
8. A. Shahar, C. E. Manning, E. D. Young, *Earth Planet. Sci. Lett.* **268**, 330 (2008).
9. R. Schoenberg, F. von Blanckenburg, *Earth Planet. Sci. Lett.* **252**, 342 (2006).

10. F. Poitrasson, R. Frey, *Chem. Geol.* **222**, 132 (2005).
11. R. T. Helz, in *Magmatic Processes: Physicochemical Principles*, B. O. Mysen, Ed. (Geochemical Society, University Park, PA, 1987), vol. 1, pp. 241–258.
12. Materials, methods, data, and modeling details are available as supporting material on Science Online.
13. V. B. Polyakov, R. N. Clayton, J. Horita, S. D. Mineev, *Geochim. Cosmochim. Acta* **71**, 3833 (2007).
14. E. A. Schauble, in *Geochemistry of Non-Traditional Stable Isotopes*, C. M. Johnson, B. L. Beard, F. Albarède, Eds. (Mineralogical Society of America, Washington, DC, 2004), vol. 55, pp. 65–111.
15. N. Dauphas, O. Rouxel, *Mass Spectrom. Rev.* **25**, 515 (2006).
16. F. M. Richter, *Geochim. Cosmochim. Acta* **71**, A839 (2007).
17. F. Huang, C. C. Lundstrom, A. J. Iannò, *Geochim. Cosmochim. Acta* **71**, A422 (2007).
18. R. T. Helz, H. Kirschenbaum, J. W. Marinenko, *Geol. Soc. Am. Bull.* **101**, 578 (1989).
19. A. D. Anbar, J. E. Roe, J. Barling, K. H. Nealson, *Science* **288**, 126 (2000).
20. F. M. Richter, E. B. Watson, R. A. Mendybaev, F.-Z. Teng, P. E. Janney, *Geochim. Cosmochim. Acta* **72**, 206 (2008).
21. R. T. Helz, C. R. Thornber, *Bull. Volcanol.* **49**, 651 (1987).
22. A. Jambon, *Geochim. Cosmochim. Acta* **44**, 1373 (1980).
23. R. T. Helz, *U.S. Geol. Surv. Prof. Pap.* **1350**, 691 (1987).
24. H. C. Urey, *J. Chem. Soc. (London)* **1947**, 562 (1947).
25. H. M. Williams *et al.*, *Science* **304**, 1656 (2004).
26. D. H. Richter, J. P. Eaton, K. J. Murata, W. U. Ault, H. L. Krivoy, *U.S. Geol. Surv. Prof. Pap.* **537-E**, 1 (1970).
27. R. T. Helz, H. Kirschenbaum, J. W. Marinenko, R. Qian, *U.S. Geol. Surv. Open-File Rep.* **94-684**, 1 (1994).
28. Discussions with S. Huang, A. T. Anderson Jr., F. M. Richter, M. Wadhwa, P. B. Tomascak, R. J. Walker, and A. Pourmand are appreciated. We thank three anonymous reviewers for constructive comments. This work was supported by a Packard fellowship, the France Chicago Center, and NASA through grant NNG06GG75G to N.D.

#### Supporting Online Material

www.sciencemag.org/cgi/content/full/320/5883/1620/DC1  
SOM Text S1 to S5  
Fig. S1  
Tables S1 to S4  
References

29 February 2008; accepted 12 May 2008  
10.1126/science.1157166

## Natural Variability of Greenland Climate, Vegetation, and Ice Volume During the Past Million Years

Anne de Vernal\* and Claude Hillaire-Marcel

The response of the Greenland ice sheet to global warming is a source of concern notably because of its potential contribution to changes in the sea level. We demonstrated the natural vulnerability of the ice sheet by using pollen records from marine sediment off southwest Greenland that indicate important changes of the vegetation in Greenland over the past million years. The vegetation that developed over southern Greenland during the last interglacial period is consistent with model experiments, suggesting a reduced volume of the Greenland ice sheet. Abundant spruce pollen indicates that boreal coniferous forest developed some 400,000 years ago during the “warm” interval of marine isotope stage 11, providing a time frame for the development and decline of boreal ecosystems over a nearly ice-free Greenland.

The potential for sea-level rise, caused by melting of the Greenland ice-sheet as surface air temperature increases, is considerable (1). Although there is evidence that the

velocity of ice streams flowing into the ocean and the rate of thinning of the ice have increased recently (2, 3), large uncertainties remain about the long-term stability of the ice sheet. The climate